ACS OMEGA

http://pubs.acs.org/journal/acsodf

Article

Synthesis and Electrochemistry of Novel Dumbbell-Shaped Bis-pyrazolino[60]fullerene Derivatives Formed Using Microwave Radiation

Mohammad H. BinSabt,* Hamad M. Al-Matar,* Alan L. Balch, and Mona A. Shalaby

Cite This: *ACS Omega* 2021, 6, 20321−20330

Read Online

ACCESS | Metrics & More | Article Recommendations | Supporting Information

ABSTRACT: The design of covalently linked [60]fullerene dimers has gained increased attention, as the linked electron donors or acceptors are in close proximity to the surface of the C_{60}, providing a valuable approach to novel molecular electronic devices. Herein, new compounds involving C_{60} dumbbells covalently connected by the π-conjugated system from azobenzene and diaryl ether linkers were synthesized following the bifunctional cycloaddition reactions to C_{60} using microwave radiation. The structural identity of the fullerene dimers has been determined using spectroscopic techniques including Fourier transform infrared (FT-IR), matrix-assisted laser desorption ionization time-of-flight (MALDI-TOF), and NMR spectroscopy, and the photophysical and the electrochemical properties for the new dumbbells have been examined using UV−vis spectroscopy, fluorescence spectroscopy, cyclic voltammetry, and square wave voltammetry. Both new dimers show electronic interaction with the fullerene cage and higher electron affinity than the pristine C_{60}.

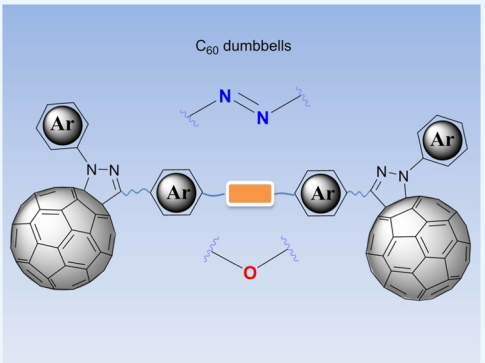

INTRODUCTION

The discovery of fullerenes in 1985[1] and the subsequent isolation[2] present the first phase of fullerene chemistry, which has expanded to many fields and produced many new compounds. As a consequence of their unique physicochemical properties originating from their high symmetries and extended conjugated π-systems, fullerenes and related analogues have inspired researchers to design new fullerene-based structures. [60]-Fullerene (C_{60}) is considered the most iconic interstellar one among the family of fullerenes and is marked as a perfect icosahedral π framework.[2] This promising class of molecules is considered the state-of-art material in many applications such as materials science,[3] biology,[4,5] antiviral therapy,[6] and photodynamic therapy (PDT) for the treatment of multiple diseases, including mainly cancer,[7,8] as acceptor and cathode buffer layer materials for organic and perovskite solar cells,[9] biosensors, catalysts,[10] and in organic chemistry.[11−15] Also, fullerene derivatives have been used to suppress the human immunodeficiency virus (HIV), influenza, and hepatitis C viruses via the inhibition of viral enzymes.[16−18] Moreover, C_{60} is able to act as an electron acceptor due to its dual electrophilic and nucleophilic characteristics combined with its notable redox activity.[19] However, one of the difficulties faced in using such compounds in many potential studies[20] is their insolubility in most organic and inorganic solvents.[21] This problem can be overcome by applying chemical modifications for C_{60}. On the other hand, the dumbbell-type dimeric fullerene materials with different spacers between the fullerene units represent an interesting class of molecules.[22,23] Fullerene dimers are an important, versatile class of organic functional materials not only because they are subunits for fullerene polymers, but also because they have found extensive applications as organic electronic materials for light harvesting,[24] optical switches,[25] charge separation, and photovoltaic devices[26] due to the presence of two fullerene cages in one molecule.[27−30] Dimers have gained particular interest due to the several structural variations produced by the linking organic functionalities. Fullero-triads are labeled for the platform of two C_{60} groups covalently attached to electroactive species. There is a growing interest to design and synthesize new [60]fullerene dimers for use in different areas such as molecular electronic devices[31−33] and supramolecular chemistry.[22] Hence, many synthetic protocols have been adapted to obtain novel designs with optimum properties for the intended applications. One of the most interesting architectures is the symmetric C_{60}−donor−donor−C_{60} (ADDA), where C_{60} acts as an acceptor (A). The electronic and electrochemical properties of C_{60} in these compounds are modulated to allow energy and electron transfer between the sites. Our group is interested in fulleropyrazoline

Received: April 28, 2021
Accepted: June 29, 2021
Published: July 27, 2021

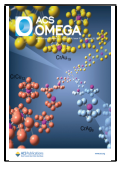

Scheme 1. Synthesis of Bis-aldehydes 5a and 5b

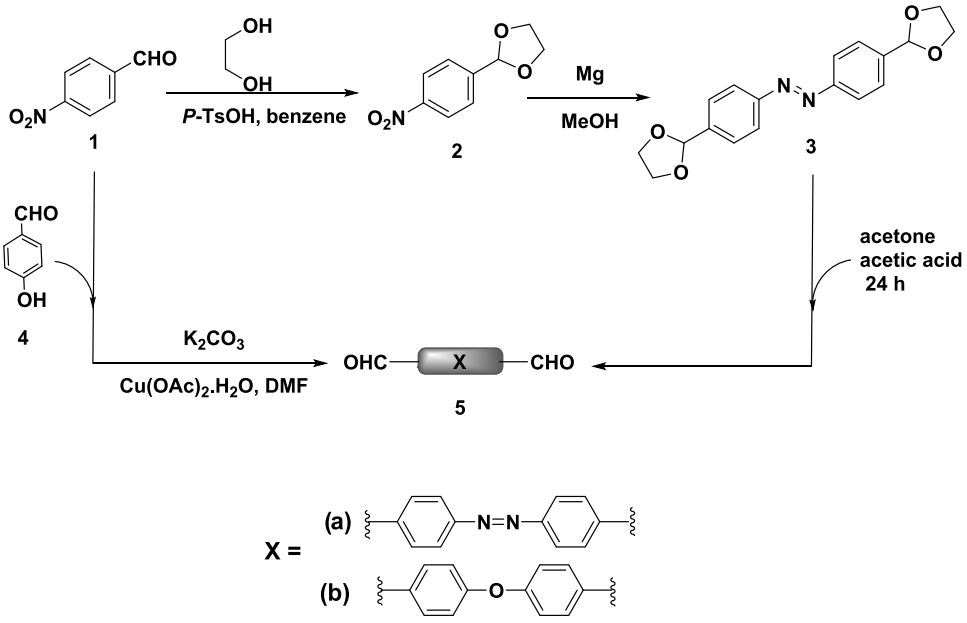

Scheme 2. Synthesis of Bis-pyrazolino[60]fullerene Triads 7a and 7b

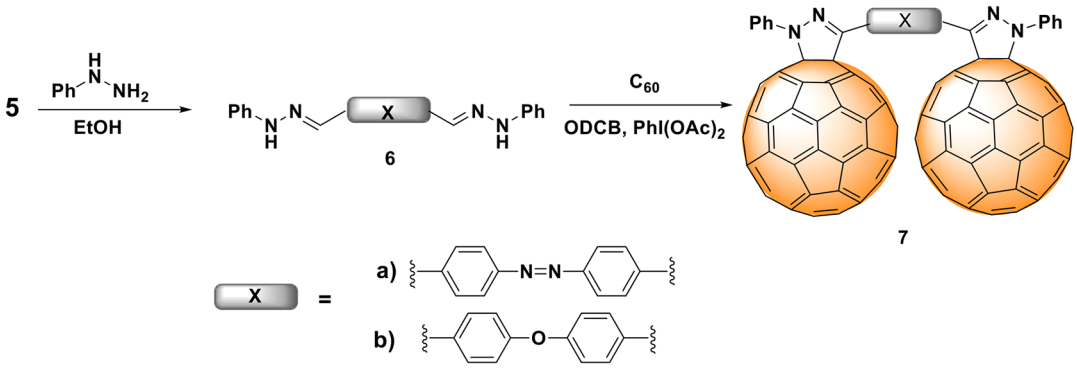

derivatives due to the enhancement of the electron affinity of these compounds that results from the inductive effect of the pyrazoline ring.[34] In addition, the pyrazoline−C_{60} unit has been found to act as a charge-separation module for the construction of photoactive and tunable devices.[35] Azobenzenes are considered as attractive classes of molecular switches in material science due to their ability to convert light into mechanical energy, which is supposed to be an essential component in future nanoscale devices.[36,37] Also, the diaryl ether structure framework is found in many biologically important natural products.[38] Recently, there has been rapid growth in the field of molecular electronics using π-conjugated linker moieties between two C_{60} end-capped structures that act as anchoring groups to form "molecular wires."[39−41] Microwave (MW) irradiation is a very useful tool in cycloaddition reactions and fullerene chemistry, where the reaction times that are required for the formation of the target compounds in synthetic organic chemistry are shorter compared to the conventional heating method.[42−44]

In this study, we used azobenzene and diaryl ether moieties as π-conjugated linkers of the central wire between two C_{60} molecules. The quest is for an economical and environment-friendly alternative synthesis methodology. Thus, we successfully prepared novel fullerene dimers using 1,3-dipolar cycloaddition of different precursors to C_{60} under microwave (MW) irradiation. Both dumbbells displayed enhanced photophysical and electrochemical properties when compared to pristine C_{60}.

RESULTS AND DISCUSSION

Synthesis. In order to prepare the symmetric dumbbell-shaped molecules consisting of the π-system between two units of C_{60}, bis-aldehyde precursors **5** were synthesized according to the strategy shown in Scheme 1. We incorporated a photoswitchable azobenzene unit and diaryl ether moiety as a bridge between the two C_{60} units. First, *p*-nitrobenzaldehyde **1** was selected to prepare our precursor compounds **5**. (*E*)-4,4′-(diazene-1,2-diyl)dibenzaldehyde **5a** was synthesized using a similar procedure reported in the literature for the synthesis of (*E*)-3,3′-(diazene-1,2-diyl)dibenzaldehyde from compound **1** under argon.[45] The spectroscopic data are in agreement with the published data for the same compound in the literature.[46] Also, 4,4′-oxydibenzaldehyde **5b** was synthesized using the cross-coupling of 4-hydroxybenzaldehyde **4** and *p*-nitrobenzaldehyde **1** by a ligand-free, copper-catalyzed method reported previously.[47] Next, the bis-hydrazones **6** were synthesized from the corresponding aldehyde compounds **1** with phenylhydrazine (Scheme 2). The structures of the bis-hydrazones **6** were characterized by NMR spectroscopy and electrospray

https://doi.org/10.1021/acsomega.1c02245
ACS Omega 2021, 6, 20321−20330

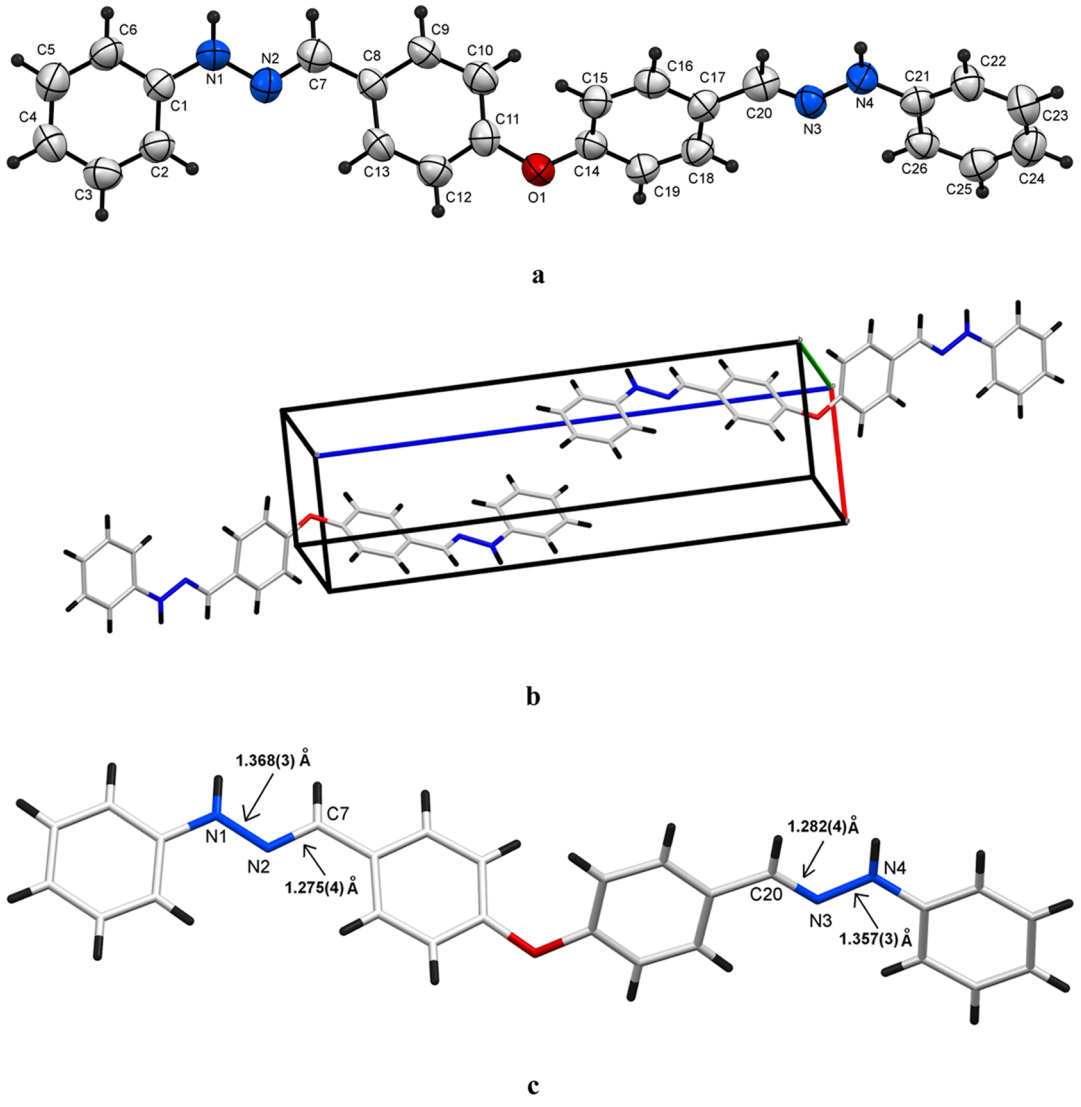

Figure 1. (a) Oak Ridge thermal ellipsoid plot (ORTEP) diagrams of the crystal structure of **6b**, (b) unit cell, and (c) crystal structure of **6b** showing N−N and C═N distances. The thermal ellipsoid is drawn at 50% probability.

ionization mass spectrometry (ESI-MS). The crystal structure of compound **6b** is illustrated in Figure 1.

The last step depends on grafting two units of C_{60} to the bis-hydrazones compound **6** by means of a double [3 + 2] cycloaddition reaction to produce the dumbbell-shaped triads compound **7** (Scheme 2), by which the dinitrile imine intermediate was generated. In order to get the bridged dimers **7**, we started our approach by using the conventional heating method, where the cycloaddition was carried out at 80 °C for 24 h (method A). Also, we examined the same reaction under microwave irradiation (200 W), where the reaction was carried out at 80 °C for 1 h to yield compounds **7** (method B). The reaction progress was monitored by thin-layer chromatography (TLC). As shown in Table 1, the microwave irradiation method (method B) was found to be better than the conventional heating method (method A) from both yield and time-consumed perspectives. The triad products **7** were purified using column chromatography (silica gel, toluene) and isolated using high-performance liquid-chromatography (HPLC) (Buckyprep, toluene).

The dumbbell compounds **7a** and **7b** show good solubility in common organic solvents such as CS_2, $CHCl_3$, and *o*-dichlorobenzene (ODCB), thus allowing the compounds to be characterized by ^1H and ^{13}C NMR, and matrix-assisted laser desorption ionization time-of-flight (MALDI-TOF) mass spectrometry, which confirmed their expected structures (see Supporting Information). Unfortunately, no exact-mass molecular ion was observed using the fast-atom bombardment (FAB) technique in both positive and negative ion modes, as it has been reported that some dumbbell compounds resist all mass spectrometric attempts, including electrospray techniques.[48]

Table 1. Synthesis of Bis-pyrazolino[60]fullerene Derivatives 7 under Conventional and Microwave Conditions

		method A[a]		method B[b]	
entry	product	yield[c] (%)	recovered C_{60} (%)	yield[c] (%)	recovered C_{60} (%)
6a	**7a**	7	71	9	56
6b	**7b**	6	72	10	71

[a]Reaction of bis-hydrazone, C_{60}, and $PhI(OAc)_2$ in *o*-dichlorobenzene (ODCB) under conventional conditions (80 °C) for 24 h. [b]Reaction of bis-hydrazone, C_{60}, and $PhI(OAc)_2$ in ODCB under microwave irradiation for 1 h. [c]Isolated yields based on the reacted C_{60}.

https://doi.org/10.1021/acsomega.1c02245
ACS Omega 2021, 6, 20321−20330

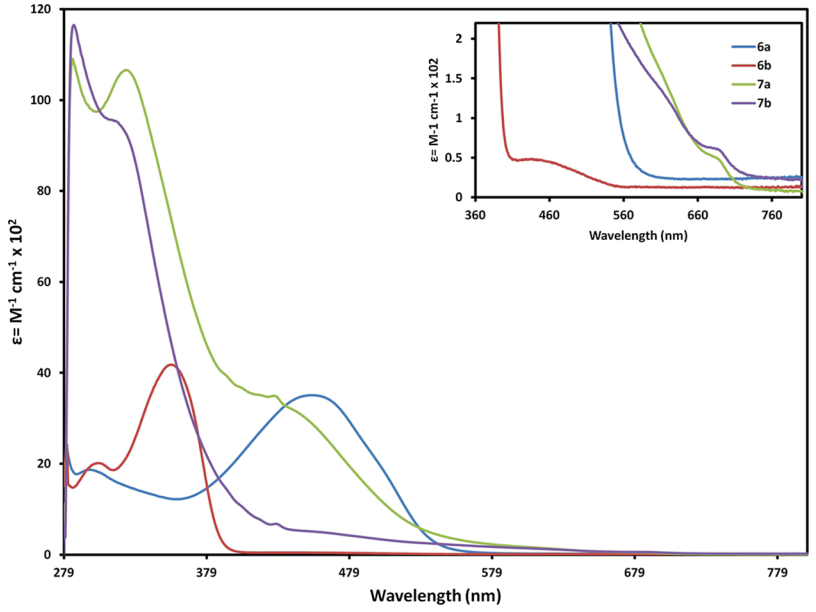

Figure 2. UV−vis spectra of **6a**, **6b**, **7a**, and **7b** in toluene solution at room temperature ($c = 1.6 \times 10^{-5}$ mol/L). The inset shows the expansion from 360 to 800 nm.

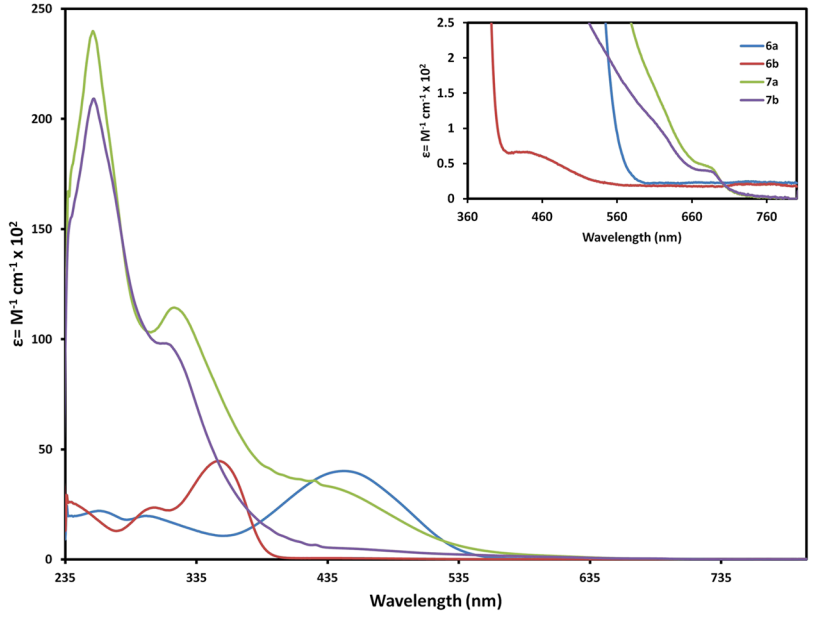

Figure 3. UV−vis spectra of **6a**, **6b**, **7a**, and **7b** in chloroform solution at room temperature ($c = 1.6 \times 10^{-5}$ mol/L). The inset shows the expansion from 360 to 800 nm.

Scheme 3. Diagram for *E*/*Z* Isomerization

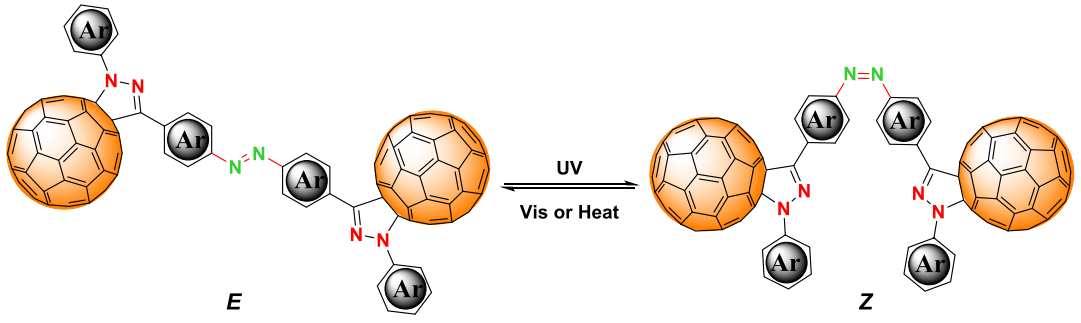

https://doi.org/10.1021/acsomega.1c02245
ACS Omega 2021, 6, 20321−20330

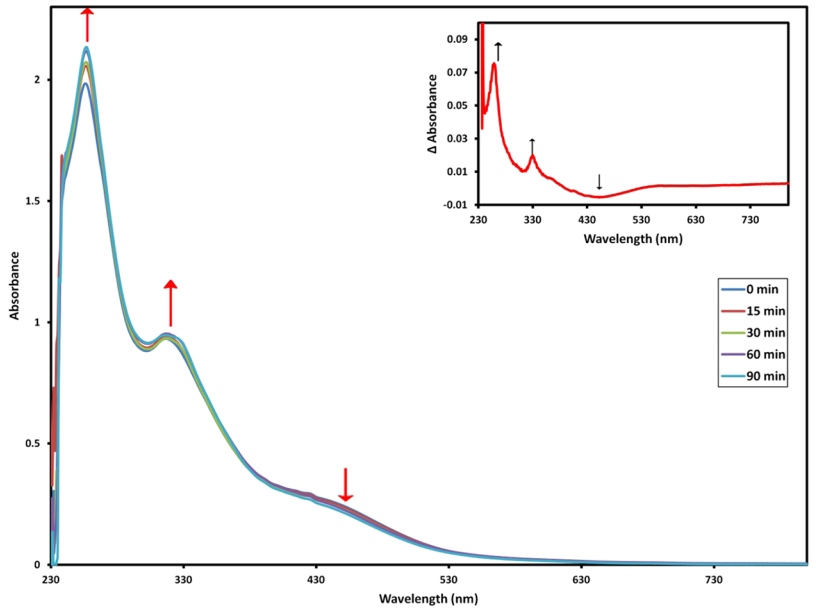

Figure 4. Absorption spectra of **7a** in chloroform solution recorded during its irradiation with UV light. (Inset) Absorption differences between **7a** before and after UV irradiation for 15 min. The arrows show the remarkable peaks of the absorption differentials.

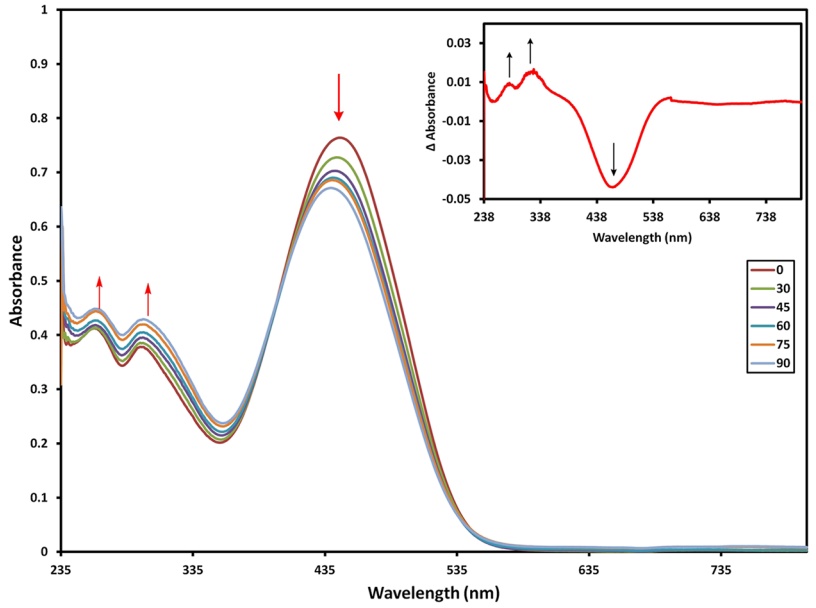

Figure 5. Absorption spectra of **6a** in chloroform solution recorded during its irradiation with UV light. (Inset) Absorption differences between **6a** before and after UV irradiation for 15 min. The arrows show the remarkable peaks of the absorption differentials.

The main molecular ion peak at m/z 720 for the C_{60} of both dumbbells was observed in FAB.

UV−Vis Spectra. The UV−vis spectra of dumbbell **7a** and **7b** compounds and their precursors **6a** and **6b** are represented in Figures 2 and 3, using toluene and chloroform as organic solvents, respectively. Both dumbbells display a main absorption band peak at 327 nm in toluene, whereas in chloroform, the peaks occur at 258 and 320 nm. In that region, the absorption bands of the fullerene overlap with the absorption bands of the central π-system. In the visible region, two absorption bands were observed for the two dumbbells in both solvents, one as a shoulder at 427 nm and the other as a weak band at 690 nm. The signal at 430 nm is characteristic for [6,6]-adducts of C_{60}.[49,50] Moreover, the maximum absorption peaks of **6a** are at 453 and 448 nm, while for **6b** they are at 354 and 352 nm in toluene and chloroform, respectively. For **6b**, a weak absorption peak was observed around 443 and 444 nm in toluene and chloroform, respectively, as shown in Figures 2 and 3.

Azobenzenes are known as useful organic dyes and photochromic molecules, where their E/Z photoisomerization generates worm-like motions.[25,51,52] The E/Z photoisomerization of **7a** is shown in Scheme 3. It is known that the E isomer is the most stable, and the two photochemical conversions for many azobenzenes occur on the scale of picoseconds, while the thermal relaxation of the Z isomer to the E isomer is much slower (milliseconds to days).[53] The azo fullerene compound **7a** has the maximum absorption band at 320 nm with a shoulder at 450 nm arising from $\pi-\pi^*$ and $n-\pi^*$ transitions, respectively.

https://doi.org/10.1021/acsomega.1c02245
ACS Omega 2021, 6, 20321−20330

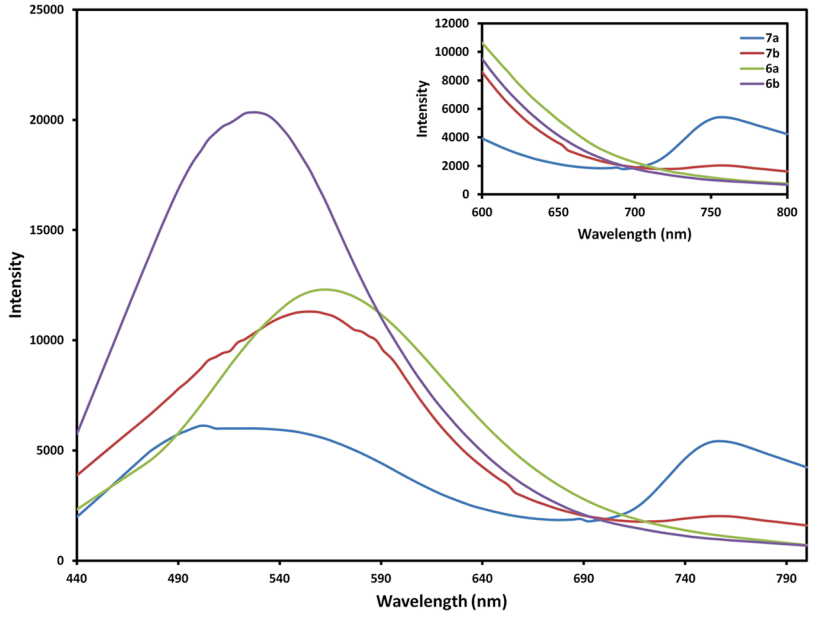

Figure 6. Fluorescence spectra of **7a** and **7b** in toluene at room temperature (the concentrations are kept at 1.6×10^{-5} mol/L; λ_{ex} = 430 nm). The inset shows the expansion from 500 to 800 nm.

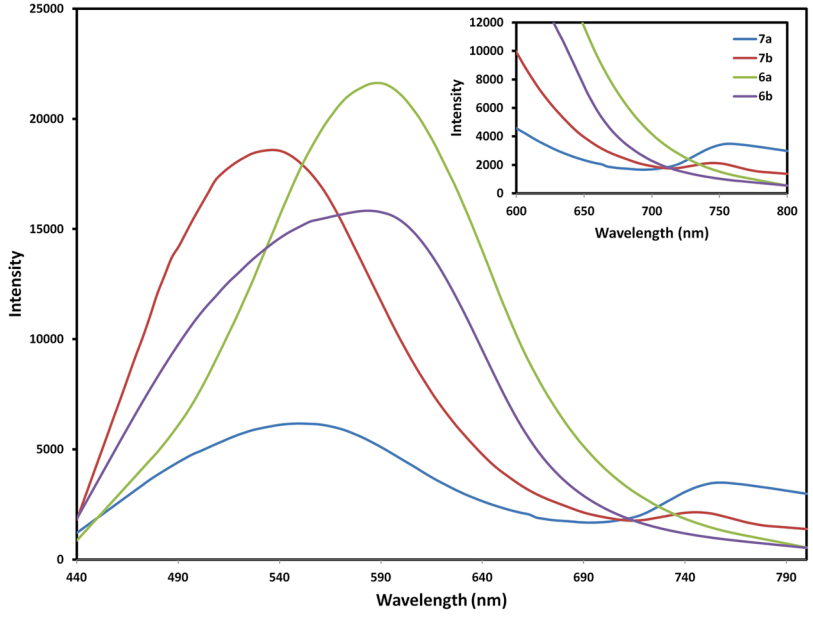

Figure 7. Fluorescence spectra of **7a** and **7b** in chloroform at room temperature (the concentrations are kept at 1.6×10^{-5} mol/L; λ_{ex} = 430 nm). The inset shows the expansion from 500 to 800 nm.

The shoulder at 450 nm showed that the *E* isomer had an elongating π-conjugation length and a lower band-gap energy of $\pi-\pi^*$ transition. A UV light radiation at 365 nm was used to switch the *E* isomer to *Z* isomer.[53] Figure 4 illustrates the absorption spectra of compound **7a** irradiated at 365 nm at room temperature and for different times in chloroform. As the time of irradiation increased from 0 to 90 min, the absorption band at around 452 nm slightly decreased while the other two bands at 330 and 259 nm gradually increased. The inset of Figure 4 shows the differences between the absorption values of **7a** before and after UV irradiation for 15 min. The partial decrease in the absorbance peak at 450 nm is due to the formation of the *Z* product with a relatively poor π-conjugation system.[51,54] Figure 5 illustrates the absorption spectra of compound **6a** irradiated at 365 nm at room temperature and for different times in chloroform. A similar behavior was found for the parent compound **6a**: as the time of irradiation increased from 0 to 90 min, the absorption band at around 464 nm slightly decreased while the other two bands at 331 and 283 nm gradually increased.

Fluorescence Spectra. The emission properties of the dumbbell compounds **7a** and **7b** and the corresponding hydrazones **6a** and **6b** were investigated to examine the possible electronic communication between the central unit of the dumbbells and the C_{60} moieties. The fluorescence spectra of **7a** and **7b** were recorded in toluene and chloroform at room temperature using a 430 nm excitation wavelength, where the excited state (S_1) of C_{60} moiety ($^1C_{60}$*) was generated. Also, the

https://doi.org/10.1021/acsomega.1c02245
ACS Omega 2021, 6, 20321−20330

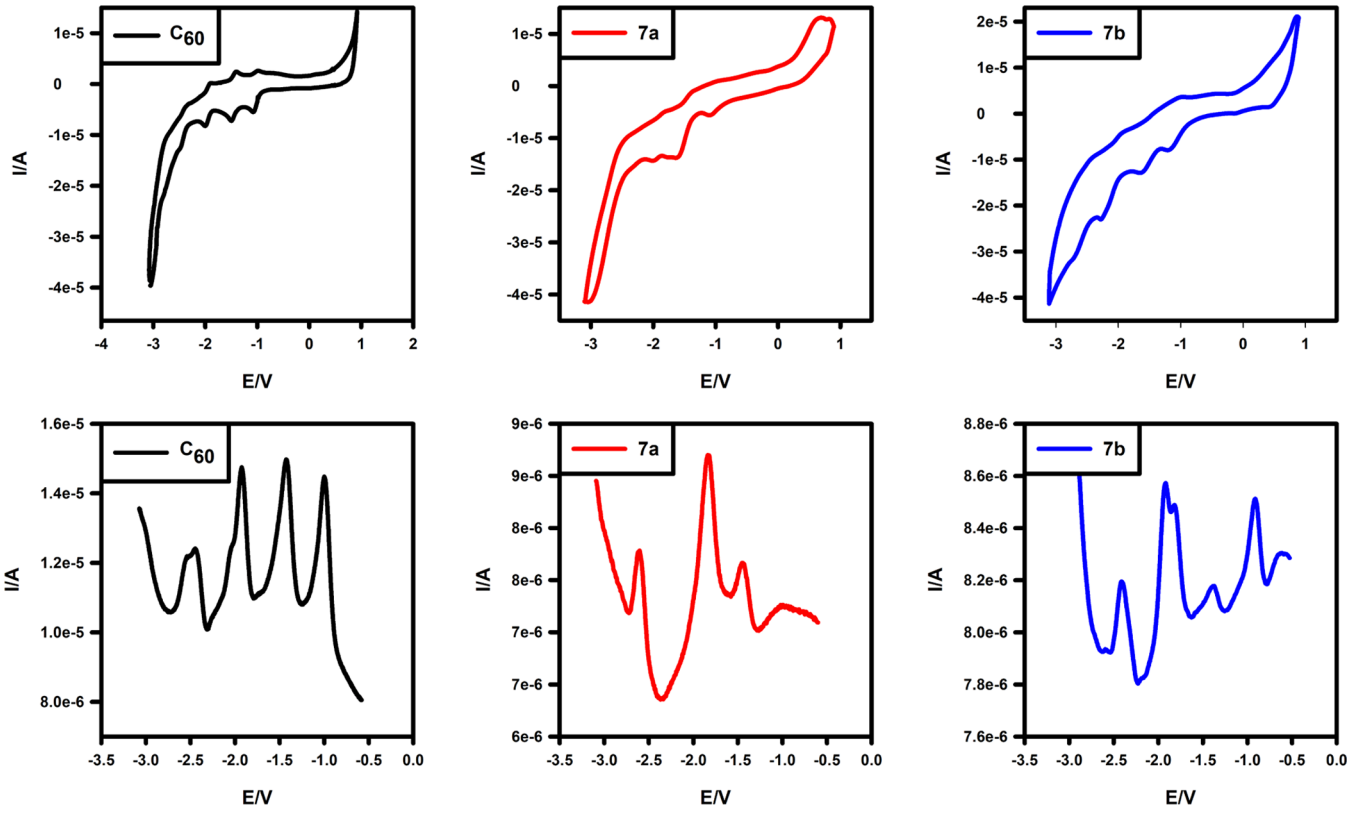

Figure 8. CV of C_{60} and dumbbells **7a** and **7b** (top), and SWV (bottom) in toluene/CH_3CN (4:1) and 0.1 M TBAP; V vs Fc/Fc^+; scan rate was 100 mV/s.

fluorescence spectra of hydrazones **6a** and **6b** were recorded at the same wavelength. The fluorescence peaks of compounds **6a** are at 556 and 587 nm, while for **6b**, they are at 526 and 584 nm in toluene and chloroform, respectively. The observed fluorescence peaks for **7a** and **7b** at around 550 nm are due to the emission of the linkers between the two fullerene moieties. Significant quenching for **7a** in the fluorescence peak intensity at around 550 nm was observed in chloroform more than in toluene, suggesting an electronic communication between the donor addend and the C_{60} moieties. For dumbbell **7b**, the fluorescence peak intensity at around 550 nm was quenched in toluene, while in chloroform no quenching was observed at 550 nm. A second observed fluorescence peak was observed at 756 nm for **7a** due to the fullerene moiety, while it was totally quenched for **7b** in both solvents, as shown in Figures 6 and 7. The observed quenching at 756 nm for **7b** may be due to the charge separation process.[55]

Electrochemistry. The electrochemical properties of C_{60} and triads **7a** and **7b** were studied by cyclic voltammetry (CV) and square wave voltammetry (SWV) at room temperature using tetrabutylammonium perchlorate (TBAP) as a supporting electrolyte in toluene/acetonitrile (ACN) (4:1) as the solvent. The resulting CV and SWV data are depicted in Figure 8 and listed in Table 2. Also, the electrochemical properties of the hydrazones **6a** and **6b** were studied by CV. As a general feature on the reduction side, both triads **7a** and **7b** showed four reduction waves, which are assigned to the successive reductions of the C_{60} cage. In order to investigate the effect of the central substituents group linked to the carbon atom of the two pyrazolino systems (C-3), while benzene rings are located on the N-1 side of the same ring systems on both sides of the central group, the first reduction potentials (E^1_{red}) were studied.

Table 2. Redox Potentials of C_{60} and Dumbbells 7a and 7b Determined by SWV[a]

	E^1_{red}	E^2_{red}	E^3_{red}	E^4_{red}	E^1_{ox}
7a	−0.948	−1.479	−1.849	−2.629	0.606[b]
6a			−1.804	−2.1952	0.452[b]
7b	−0.915	−1.417	−1.841 (−1.931)	−2.426	0.401[b]
6b		−1.532			0.354[b]
C_{60}	−1.001	−1.424	−1.907	−2.449	

[a]Experimental conditions: *V* vs ferrocene/ferrocenium (Fc/Fc^+); the reference electrode is Ag/AgCl; the working electrode is a glassy carbon electrode (GCE); 0.1 M nBu_4NClO_4; scan rate: 100 mV/s; measured in toluene/CH_3CN (4:1 v/v) at room temperature. [b]Measured by CV.

Interestingly, unlike the standard behavior found in most of the C_{60} derivatives that showed reduction potentials shifted to more negative values,[56] both triads **7a** and **7b** show an anodic shift to more positive values (53−86 mV) relative to the pristine C_{60} due to the negative inductive effect (−*I*) of the pyrazoline ring,[57] as shown in Table 2. Consequently, both triads **7a** and **7b** show a higher electron affinity than the parent C_{60}. In the anodic region, the first oxidation E^1_{ox} values of **7a** and **7b**, attributed to the organic addend linked with C_{60}, are positively shifted by 154 and 47 mV, respectively, compared to the hydrazones **6a** and **6b**, suggesting the existence of some electronic interaction with the fullerene cage.

CONCLUSIONS

We have synthesized a new series of dumbbell-shaped compounds via [3 + 2] cycloaddition reaction mediated with $PhI(OAc)_2$ as an oxidant and enhanced by microwave radiation.

https://doi.org/10.1021/acsomega.1c02245
ACS Omega 2021, 6, 20321−20330

The formed compounds were investigated using Fourier transform infrared (FT-IR), MALDI-TOF, NMR, UV−vis, fluorescence spectra, and electrochemical properties. According to the first reduction potential, both dumbbells showed an improved electron acceptor ability than the pristine C_{60} in the ground state, which is important for further applications in the preparation of optoelectronic devices. Also, the fluorescence data at λ_{ex} = 430 nm for dumbbell **7b** show a complete quenching at about 750 nm compared to the dumbbell **7a**, and a significant quenching for **7a** at about 550 nm was observed in chloroform, more than in toluene, indicating an electronic communication between the donor addend and C_{60} moieties. These compounds are potentially useful for applications in material science; hence, the photophysical and photochemical measurements of both compounds will be studied.

EXPERIMENTAL SECTION

General Methods. All cycloaddition reactions were performed in standard glassware under an inert atmosphere of argon. C_{60} was purchased from Sigma-Aldrich. All solvents used in this study were purchased from Aldrich. Thin-layer chromatography (TLC) was performed using Polygram SIL G/UV 254 TLC plates, and visualization was performed under ultraviolet light at 254 and 365 nm. Column chromatography was performed using Merck silica gel 60 of mesh size 0.040−0.063 mm. Melting points were recorded using a Griffin melting point apparatus and are reported unmodified. Mass analyses were done by electron impact (EI) and fast-atom bombardment (FAB) using a Thermo DFS mass spectrometer. High-resolution mass spectrometry (HRMS) analysis was performed using a Xevo G2-S QTof mass spectrometer. IR spectra were obtained using a JASCO 6300 FT-IR. The clusters of peaks that corresponded to the calculated isotope compositions of the molecular ions were observed by matrix-assisted laser desorption/ionization mass spectrometry (MALDI-TOF) via an ultrafleXtreme (Bruker). ^{1}H NMR (600 MHz) and ^{13}C NMR (150 MHz) spectra were recorded at 25 °C using a Bruker DPX 600 superconducting NMR spectrometer. UV−vis studies were performed using a Varian Cary 5 spectrometer from Agilent. Fluorescence measurements were carried out with Horiba Jobin Yvon-Fluoromax-4 equipped with a time-correlated single-photon-counting (TCSPC) module. Single-crystal data collections were performed on a Rigaku R-Axis Rapid diffractometer using filtered Mo Kα radiation. The diffraction data were collected at a temperature of −123 °C (Oxford Cryosystems). Microwave experiments were carried out using a CEM Discover LabMate microwave apparatus (300 W with ChemDriver software; Matthews, NC). The reactions were conducted under microwave irradiation in heavy-walled Pyrex tubes fitted with PCS caps (closed vessels under pressure). Irradiation experiments of the $E \rightarrow Z$ photoisomerization were performed using ultraviolet light at 365 nm with the model UVGL-85 (6 W) at room temperature (23 °C), where the intensity of light is 1200 μW/cm^2, a Waters HPLC instrument equipped with a pump (Waters 1525EF), and a UV/visible detector (Waters 2487). The chromatographic separation was carried out in a cosmosil buckyprep HPLC column (10 × 250 mm^2). HPLC separations were performed by injecting 1000 μL with an isocratic toluene mobile phase at a flow rate of 2 mL/min. Cyclic voltammetry measurements were carried out on a Gamry Instruments reference 3000 potentiostat using Ag/0.01 M AgCl (model 6.0733.100, Metrohm), 0.1 M TBAP in ACN as the reference electrode, an auxiliary electrode consisting of a Pt sheet, and a MF-2012 glassy carbon electrode (3 mm) as the working electrode, directly immersed in the solution. Ferrocene (Fc) was added as an internal reference and all of the potentials were referenced relative to the Fc/Fc$^+$ couple. $E_{1/2}$ values were taken as the average of the anodic and cathodic peak potentials. Scan rate: 100 mV/s.

Synthesis. *Synthesis of Bis-aldehyde Precursors (**5a** and **5b**).* They were synthesized as reported in the literature.[45−47]

*General Synthesis Procedure of the Substituted Bis-hydrazones (**6a** and **6b**).* These compounds were obtained by mixing 1 molar equiv of the corresponding bis-aldehyde **5** and 2 molar equiv of phenylhydrazine in ethanol under reflux conditions for 5 h. The precipitated bis-hydrazones were filtered, washed, and recrystallized from ethanol.

*Bis-hydrazone (**6a**).* Red color; m.p. 233−236 °C; FT-IR (KBr) ν (cm^{-1}) 3428.8, 3309.2, 3035.4, 1592.9. ^{1}H NMR (dimethyl sulfoxide (DMSO)) δ 6.79 (m, 2H), 7.12 (d, 4H, J = 7.8 Hz), 7.24 (t, 4H, 3.6), 7.80−7.93 (m, 8H), 8.21−8.28 (m, 2H), 10.65 (s, 2H, D_2O exchange); ^{13}C NMR (DMSO) δ 112.2, 119.3, 123.1, 126.3, 129.1, 135.1, 138.8, 144.8, 151.2; MS (EI, 70 eV): m/z (%) = 418.3 (M$^+$, 100); HRMS (EI): m/z calcd for $C_{26}H_{23}N_6$: 419.1984; found: 419.2182.

*Bis-hydrazone (**6b**).* Orange color; m.p. 216−218 °C; FT-IR (KBr) ν (cm^{-1}) 3444.2, 3305.3, 3035.4, 1595.8. ^{1}H NMR (DMSO) δ 6.73 (t, 2H, 7.2 Hz), 7.06 (m, 8H), 7.21 (t, 4H, 8.4 Hz), 7.68 (d, 4H, 8.4 Hz), 7.87 (s, 2H), 10.30 (s, 2H, D_2O exchange); ^{13}C NMR (DMSO) δ 111.8, 118.4, 118.7, 127.1, 128.9, 131.3, 135.7, 145.2, 156.2; MS (EI, 70 eV): m/z (%) = 406.3 (M$^+$, 100); HRMS (EI): m/z calcd for $C_{26}H_{23}N_4O$: 407.1872; found: 407.2042.

*General Synthesis Procedure of the Bis-cycloadducts (**7a** and **7b**).* **Method A**: A mixture of C_{60} (124 mg, 0.172 mmol), substituted hydrazones (**6a** and **6b**) (0.068 mmol), and PhI(OAc)$_2$ (0.068 mmol) was dissolved in 10 mL of ODCB and stirred at 80 °C overnight. The reaction progress was monitored by TLC with toluene as an eluent. At the end of the reaction, hexane was added, and the precipitate was filtered and then purified on a silica gel column using toluene as eluent to afford the adducts (**7a** and **7b**). The reaction products **7a** and **7b** were separated by HPLC using toluene as an eluent.

Method B: Using a similar process, the mixture was irradiated by microwave irradiation (200 W) for 1 h at 60 °C.

*Compound **7a**.* Dark orange solid; FT-IR (KBr) ν (cm^{-1}) 3432.6, 1704.7, 1631.4, 1596.7, 1492.63, 1452.1, 1253.5, 1191.7, 1137.8, 848.5, 802.2, 690.3, 526.4. ^{1}H NMR ($CDCl_3$) δ 7.307 (t, 1H, J = 7.8 Hz), 7.52 (t, 2H, J = 7.8 Hz), 7.60−7.65 (m, 3H), 7.99 (d, 2H, J = 7.8 Hz), 8.04−8.07 (m, 4H), 8.12 (d, 2H, J = 9 Hz), 8.26 (d, 2H J = 8.4 Hz), 8.55 (d, 2H, J = 9 Hz); ^{13}C NMR ($CDCl_3$) δ 156.0, 152.6, 152.3, 147.8, 147.4, 146.6, 146.5, 146.2, 146.1, 146.0, 145.6, 145.4, 145.3, 145.1, 144.6, 144.4, 143.3, 143.1, 143.0, 142.8, 142.6, 142.4, 142.3, 142.0, 140.5, 139.9, 136.7, 136.5, 136.2, 133.9, 132.7, 131.9, 130.9, 130.7, 130.4, 129.6, 127.9, 125.8, 124.3, 124.0, 123.7, 123.1. UV−vis (toluene) λ_{max} (nm) (ε) 686 (50.08), 427 (3495.16), 327 (10 539.95), 286 (10 804.29); UV−vis ($CHCl_3$) λ_{max} (nm) (ε) 686 (43.98), 427 (3526.59), 327 (10 964.82), 320 (11 403.66), 258 (11 945.6). FAB-MS m/z: 918, 720 (C_{60}). MALDI-TOF mass: calcd 1855.162, found 1854.927 (M − H)$^+$.

*Compound **7b**.* Brown solid; FT-IR (KBr) ν (cm^{-1}) 3423.9, 1704.7, 1661.3, 1591.9, 1495.5, 1451.1, 1241.9, 1192.7, 1165.7, 879.3, 691.3, 527.4. ^{1}H NMR ($CDCl_3$) δ 7.07−7.11 (m, 2H), 7.14−7.19 (m, 3H), 7.40 (t, 2H, J = 8.4 Hz), 7.48−7.53 (m, 3H), 7.86 (m, 2H), 7.91−7.93 (m, 2H), 8.00 (d, 1H, J = 7.8 Hz),

https://doi.org/10.1021/acsomega.1c02245
ACS Omega 2021, 6, 20321−20330

8.02 (d, 1H, J = 8.4 Hz), 8.27 (d, 2H, J = 7.8 Hz); ^{13}C NMR ($CDCl_3$) δ 152.2, 147.7, 147.4, 146.5, 146.4, 146.2, 146.1, 146.0, 145.9, 145.6, 145.4, 145.3, 144.9, 144.6, 144.4, 143.3, 143.2, 143.0, 142.5, 142.4, 142.3, 142.0, 140.5, 139.9, 136.7, 136.4, 133.7, 133.2, 132.2, 130.8, 129.5, 129.1, 126.0, 125.5, 124.1, 123.8, 120.4, 119.3, 118.3. UV−vis (toluene) λ_{max} (nm) (ε) 686 (61.45), 427 (680.39), 327 (8895.45), 286 (11 653.63); UV−vis ($CHCl_3$) λ_{max} (nm) (ε) 686 (38.80), 427 (646.08), 327 (8437.34), 320 (9333.77), 258 (12 341.88). FAB-MS m/z: 1808, 720 (C_{60}), MALDI-TOF mass: calcd 1843.151, found 1834.934 $(M - O + 7H)^+$.

■ ASSOCIATED CONTENT

Supporting Information

The Supporting Information is available free of charge at https://pubs.acs.org/doi/10.1021/acsomega.1c02245.

^{1}H NMR spectra, ^{13}C NMR spectra, HRMS, H−H correlated spectroscopy (COSY) NMR spectra, H−H nuclear Overhauser enhancement spectroscopy (NOESY), heteronuclear single quantum coherence (HSQC) spectra, heteronuclear multiple bond correlation (HMBC) spectra, MALDI-TOF spectra, and HPLC chromatograms of compounds **5a**, **5b**, **6a**, **6b**, **7a**, and **7b**; experimental details and crystal data for the compound **6b** (Table S1) (PDF)

Crystallographic data (CIF)

■ AUTHOR INFORMATION

Corresponding Authors

Mohammad H. BinSabt − *Chemistry Department, Faculty of Science, University of Kuwait, Safat 13060, Kuwait;* orcid.org/0000-0003-4057-233X; Phone: +965 24985587; Email: mohammad.binsabt@ku.edu.kw; Fax: +965 24816482

Hamad M. Al-Matar − *Chemistry Department, Faculty of Science, University of Kuwait, Safat 13060, Kuwait;* Phone: +965 24987559; Email: h.almatar@ku.edu.kw; Fax: +965 24816482

Authors

Alan L. Balch − *Department of Chemistry, University of California at Davis, Davis, California 95616, United States;* orcid.org/0000-0002-8813-6281

Mona A. Shalaby − *Chemistry Department, Faculty of Science, University of Kuwait, Safat 13060, Kuwait*

Complete contact information is available at: https://pubs.acs.org/10.1021/acsomega.1c02245

Notes

The authors declare no competing financial interest.

CCDC 2068874 contains the supplementary crystallographic data for this paper. These data can be obtained free of charge from the Cambridge Crystallographic Data Centre via www.ccdc.cam.ac.uk/structures.

■ ACKNOWLEDGMENTS

This research work was financially supported by the University of Kuwait through a research grant (SC12/18). The RSP unit general facilities of the Faculty of Science (GFS) supported by research grants GS01/05, GS01/03, GS03/01, GS02/01, and GS03/08 are greatly appreciated. The authors thank the Chemistry Department at Kuwait University for the use of the MALDI-TOF mass spectrometer.

■ REFERENCES

(1) Kroto, H. W.; Heath, J. R.; O'Brien, S. C.; Curl, R. F.; Smalley, R. E. C60: Buckminsterfullerene. *Nature* **1985**, *318*, 162−163.

(2) Krätschmer, W.; Lamb, L. D.; Fostiropoulos, K.; Huffman, D. R. Solid C60: a new form of carbon. *Nature* **1990**, *347*, 354−358.

(3) Montellano López, A.; Mateo-Alonso, A.; Prato, M. Materials chemistry of fullerene C60 derivatives. *J. Mater. Chem.* **2011**, *21*, 1305−1318.

(4) Haddon, R. C. Chemistry of the Fullerenes: The Manifestation of Strain in a Class of Continuous Aromatic Molecules. *Science* **1993**, *261*, 1545.

(5) Haddon, R. C. Electronic structure, conductivity and superconductivity of alkali metal doped (C60). *Acc. Chem. Res.* **1992**, *25*, 127−133.

(6) Cataldo, F.; Da Ros, T. *Medicinal Chemistry and Pharmacological Potential of Fullerenes and Carbon Nanotubes*; Springer Science & Business Media, 2008; Vol. *1*, pp 1−408.

(7) Piotrowski, P.; Jakubow, K.; Kowalewska, B.; Kaim, A. Dioxygen insensitive C70/AuNPs hybrid system for rapid and quantitative glucose biosensing. *RSC Adv.* **2017**, *7*, 45634−45640.

(8) Gross, S.; Gilead, A.; Scherz, A.; Neeman, M.; Salomon, Y. Monitoring photodynamic therapy of solid tumors online by BOLD-contrast MRI. *Nat. Med.* **2003**, *9*, 1327−1331.

(9) Taylor, R. C60, C70, C76, C78 and C84: numbering, π-bond order calculations and addition pattern considerations. *J. Chem. Soc., Perkin Trans. 2* **1993**, 813−824.

(10) Chang, C.-L.; Hu, C.-W.; Tseng, C.-Y.; Chuang, C.-N.; Ho, K.-C.; Leung, M.-k. Ambipolar Freestanding Triphenylamine/Fullerene Thin-film by Electrochemical Deposition and Its Read-Writable Properties by Electrochemical Treatments. *Electrochim. Acta* **2014**, *116*, 69−77.

(11) Hirsch, A.; Brettreich, M. *Fullerenes: Chemistry and Reactions*; John Wiley & Sons, 2006.

(12) Martín, N. New challenges in fullerene chemistry. *Chem. Commun.* **2006**, 2093−2104.

(13) Tzirakis, M. D.; Orfanopoulos, M. Radical Reactions of Fullerenes: From Synthetic Organic Chemistry to Materials Science and Biology. *Chem. Rev.* **2013**, *113*, 5262−5321.

(14) Zhu, S.-E.; Li, F.; Wang, G.-W. Mechanochemistry of fullerenes and related materials. *Chem. Soc. Rev.* **2013**, *42*, 7535−7570.

(15) Xiao, S.; Xu, J.-H.; Li, Y.-S.; Du, C.-M.; Li, Y.-L.; Jiang, L.; Zhu, D. Preparation and characterization of a novel dumbbell-type [60]-fullerene dimer containing a cyanine dye. *New J. Chem.* **2001**, *25*, 1610−1612.

(16) Friedman, S. H.; DeCamp, D. L.; Sijbesma, R. P.; Srdanov, G.; Wudl, F.; Kenyon, G. L. Inhibition of the HIV-1 protease by fullerene derivatives: model building studies and experimental verification. *J. Am. Chem. Soc.* **1993**, *115*, 6506−6509.

(17) Shoji, M.; Takahashi, E.; Hatakeyama, D.; Iwai, Y.; Morita, Y.; Shirayama, R.; Echigo, N.; Kido, H.; Nakamura, S.; Mashino, T.; et al. Anti-influenza activity of c60 fullerene derivatives. *PLoS One* **2013**, *8*, No. e66337.

(18) Kataoka, H.; Ohe, T.; Takahashi, K.; Nakamura, S.; Mashino, T. Novel fullerene derivatives as dual inhibitors of Hepatitis C virus NS5B polymerase and NS3/4A protease. *Bioorg. Med. Chem. Lett.* **2016**, *26*, 4565−4567.

(19) Okumura, M.; Mikawa, M.; Yokawa, T.; Kanazawa, Y.; Kato, H.; Shinohara, H. Evaluation of water-soluble metallofullerenes as MRI contrast agents. *Acad. Radiol.* **2002**, *9*, S495−S497.

(20) Meng, H.; Xing, G.; Sun, B.; Zhao, F.; Lei, H.; Li, W.; Song, Y.; Chen, Z.; Yuan, H.; Wang, X.; Long, J.; Chen, C.; Liang, X.; Zhang, N.; Chai, Z.; Zhao, Y. Potent Angiogenesis Inhibition by the Particulate Form of Fullerene Derivatives. *ACS Nano* **2010**, *4*, 2773−2783.

(21) Xing, G.; Yuan, H.; He, R.; Gao, X.; Jing, L.; Zhao, F.; Chai, Z.; Zhao, Y. The Strong MRI Relaxivity of Paramagnetic Nanoparticles. *J. Phys. Chem. B* **2008**, *112*, 6288−6291.

(22) Segura, J. L.; Martín, N. [60]Fullerene dimers. *Chem. Soc. Rev.* **2000**, *29*, 13−25.
(23) Zhao, H.-Q.; Yang, S.; Xu, T.-L.; Shi, X.; Lu, S.; Wu, J.-W.; Wang, C.; Hu, J.-M. Synthesis and characterization of single-bond fullerene dimer derivatives. *J. Mater. Res.* **2020**, *35*, 2676−2683.
(24) Delgado, J. L.; Espíldora, E.; Liedtke, M.; Sperlich, A.; Rauh, D.; Baumann, A.; Deibel, C.; Dyakonov, V.; Martín, N. Fullerene Dimers (C60/C70) for Energy Harvesting. *Chem. − Eur. J.* **2009**, *15*, 13474−13482.
(25) Zhang, J.; Porfyrakis, K.; Morton, J. J. L.; Sambrook, M. R.; Harmer, J.; Xiao, L.; Ardavan, A.; Briggs, G. A. D. Photoisomerization of a Fullerene Dimer. *J. Phys. Chem. C* **2008**, *112*, 2802−2804.
(26) Collavini, S.; Delgado, J. L. Fullerenes: the stars of photovoltaics. *Sustainable Energy Fuels* **2018**, *2*, 2480−2493.
(27) Giacalone, F.; Martín, N. Fullerene Polymers: Synthesis and Properties. *Chem. Rev.* **2006**, *106*, 5136−5190.
(28) Balch, A. L.; Winkler, K. Two-Component Polymeric Materials of Fullerenes and the Transition Metal Complexes: A Bridge between Metal−Organic Frameworks and Conducting Polymers. *Chem. Rev.* **2016**, *116*, 3812−3882.
(29) Wei, T.; Pérez-Ojeda, M. E.; Hirsch, A. The first molecular dumbbell consisting of an endohedral Sc3N@C80 and an empty C60-fullerene building block. *Chem. Commun.* **2017**, *53*, 7886−7889.
(30) Sabirov, D. S. Polarizability of C60 fullerene dimer and oligomers: the unexpected enhancement and its use for rational design of fullerene-based nanostructures with adjustable properties. *RSC Adv.* **2013**, *3*, 19430−19439.
(31) Tashiro, K.; Hirabayashi, Y.; Aida, T.; Saigo, K.; Fujiwara, K.; Komatsu, K.; Sakamoto, S.; Yamaguchi, K. A Supramolecular Oscillator Composed of Carbon Nanocluster C120 and a Rhodium(III) Porphyrin Cyclic Dimer. *J. Am. Chem. Soc.* **2002**, *124*, 12086−12087.
(32) Tian, C.; Kochiss, K.; Castro, E.; Betancourt-Solis, G.; Han, H.; Echegoyen, L. A dimeric fullerene derivative for efficient inverted planar perovskite solar cells with improved stability. *J. Mater. Chem. A* **2017**, *5*, 7326−7332.
(33) Jia, L.; Chen, M.; Yang, S. Functionalization of fullerene materials toward applications in perovskite solar cells. *Mater. Chem. Front.* **2020**, *4*, 2256−2282.
(34) Al-Matar, H. M.; BinSabt, M. H.; Shalaby, M. A. Synthesis and Electrochemistry of New Furylpyrazolino [60] fullerene Derivatives by Efficient Microwave Radiation. *Molecules* **2019**, *24*, No. 4435.
(35) Armaroli, N.; Accorsi, G.; Gisselbrecht, J.-P.; Gross, M.; Krasnikov, V.; Tsamouras, D.; Hadziioannou, G.; Gómez-Escalonilla, M. J.; Langa, F.; Eckert, J.-F.; Nierengarten, J.-F. Photoinduced processes in fullerenopyrrolidine and fullerenopyrazoline derivatives substituted with an oligophenylenevinylene moiety. *J. Mater. Chem.* **2002**, *12*, 2077−2087.
(36) Bléger, D.; Schwarz, J.; Brouwer, A. M.; Hecht, S. o-Fluoroazobenzenes as Readily Synthesized Photoswitches Offering Nearly Quantitative Two-Way Isomerization with Visible Light. *J. Am. Chem. Soc.* **2012**, *134*, 20597−20600.
(37) Hugel, T.; Holland, N. B.; Cattani, A.; Moroder, L.; Seitz, M.; Gaub, H. E. Single-Molecule Optomechanical Cycle. *Science* **2002**, *296*, 1103.
(38) Bedos-Belval, F.; Rouch, A.; Vanucci-Bacqué, C.; Baltas, M. Diaryl ether derivatives as anticancer agents − a review. *MedChemComm* **2012**, *3*, 1356−1372.
(39) Atienza, C.; Insuasty, B.; Seoane, C.; Martín, N.; Ramey, J.; Rahman, G. M. A.; Guldi, D. M. Connecting two C60 stoppers to molecular wires: ultrafast intramolecular deactivation reactions. *J. Mater. Chem.* **2005**, *15*, 124−132.
(40) Pålsson, L.-O.; Wang, C.; Batsanov, A. S.; King, S. M.; Beeby, A.; Monkman, A. P.; Bryce, M. R. Efficient Intramolecular Charge Transfer in Oligoyne-Linked Donor−π−Acceptor Molecules. *Chem. − Eur. J.* **2010**, *16*, 1470−1479.
(41) Li, H.; Schubert, C.; Dral, P. O.; Costa, R. D.; La Rosa, A.; Thüring, J.; Liu, S.-X.; Yi, C.; Filippone, S.; Martín, N.; Decurtins, S.; Clark, T.; Guldi, D. M. Probing Charge Transfer in Benzodifuran−C60 Dumbbell-Type Electron Donor−Acceptor Conjugates: Ground- and Excited-State Assays. *ChemPhysChem* **2013**, *14*, 2910−2919.
(42) de la Cruz, P.; de la Hoz, A.; Langa, F.; Illescas, B.; Martin, N. Cycloadditions to [60]fullerene using microwave irradiation: A convenient and expeditious procedure. *Tetrahedron* **1997**, *53*, 2599−2608.
(43) Langa, F.; de la Cruz, P.; Espíldora, E.; García, J. J.; Pérez, M. C.; de la Hoz, A. Fullerene chemistry under microwave irradiation. *Carbon* **2000**, *38*, 1641−1646.
(44) Langa, F.; la Cruz, P. Microwave Irradiation: An Important Tool to Functionalize Fullerenes and Carbon Nanotubes. *Comb. Chem. High Throughput Screening* **2007**, *10*, 766−782.
(45) Su, R.; Lü, L.; Zheng, S.; Jin, Y.; An, S. Synthesis and characterization of novel azo-containing or azoxy-containing Schiff bases and their antiproliferative and cytotoxic activities. *Chem. Res. Chin. Univ.* **2015**, *31*, 60−64.
(46) Gerstel, P.; Klumpp, S.; Hennrich, F.; Poschlad, A.; Meded, V.; Blasco, E.; Wenzel, W.; Kappes, M. M.; Barner-Kowollik, C. Highly Selective Dispersion of Single-Walled Carbon Nanotubes via Polymer Wrapping: A Combinatorial Study via Modular Conjugation. *ACS Macro Lett.* **2014**, *3*, 10−15.
(47) Chen, J.; Wang, X.; Zheng, X.; Ding, J.; Liu, M.; Wu, H. Ligand-free copper-catalyzed O-arylation of nitroarenes with phenols. *Tetrahedron* **2012**, *68*, 8905−8907.
(48) de Lucas, A. I.; Martín, N.; Sánchez, L.; Seoane, C. The first dumbbell-type C60 dimer connected by a double donor spacer. *Tetrahedron Lett.* **1996**, *37*, 9391−9394.
(49) Mitrović, A.; Stevanović, J.; Milčić, M.; Žekić, A.; Stanković, D.; Chen, S.; Badjić, J. D.; Milić, D.; Maslak, V. Fulleropyrrolidine molecular dumbbells act as multi-electron-acceptor triads. Spectroscopic, electrochemical, computational and morphological characterizations. *RSC Adv.* **2015**, *5*, 88241−88248.
(50) Lebedeva, M. A.; Chamberlain, T. W.; Schröder, M.; Khlobystov, A. N. An efficient route to the synthesis of symmetric and asymmetric diastereomerically pure fullerene triads. *Tetrahedron* **2012**, *68*, 4976−4985.
(51) Sasaki, T.; Tour, J. M. Synthesis of a New Photoactive Nanovehicle: A Nanoworm. *Org. Lett.* **2008**, *10*, 897−900.
(52) Đorđević, L.; Casimiro, L.; Demitri, N.; Baroncini, M.; Silvi, S.; Arcudi, F.; Credi, A.; Prato, M. Light-Controlled Regioselective Synthesis of Fullerene Bis-Adducts. *Angew. Chem., Int. Ed.* **2021**, *60*, 313−320.
(53) Merino, E.; Ribagorda, M. Control over molecular motion using the cis−trans photoisomerization of the azo group. *Beilstein J. Org. Chem.* **2012**, *8*, 1071−1090.
(54) Chu, C.-C.; Chang, Y.-C.; Tsai, B.-K.; Lin, T.-C.; Lin, J.-H.; Hsiao, V. K. S. trans/cis-Isomerization of Fluorene-Bridged Azo Chromophore with Significant Two-Photon Absorbability at Near-Infrared Wavelength. *Chem. − Asian J.* **2014**, *9*, 3390−3396.
(55) Oswald, F.; Chopin, S.; de la Cruz, P.; Orduna, J.; Garín, J.; Sandanayaka, A. S. D.; Araki, Y.; Ito, O.; Delgado, J. L.; Cousseau, J.; Langa, F. Through-space communication in a TTF−C60−TTF triad. *New J. Chem.* **2007**, *31*, 230−236.
(56) Oswald, F.; de la Cruz, P.; Langa, F. Nitration of fullerene derivatives under mild conditions. *Synlett* **2007**, *2007*, 1051−1054.
(57) Delgado, J. L.; de la Cruz, P.; López-Arza, V.; Langa, F.; Kimball, D. B.; Haley, M. M.; Araki, Y.; Ito, O. The Isoindazole Nucleus as a Donor in Fullerene-Based Dyads. Evidence for Electron Transfer. *J. Org. Chem.* **2004**, *69*, 2661−2668.

https://doi.org/10.1021/acsomega.1c02245
ACS Omega 2021, 6, 20321−20330